Transp Porous Med (2005) 60:33–42
DOI 10.1007/s11242-004-3250-0

Weak Non-Linear Analysis of Convection in a Gravity Modulated Porous Layer

SANESHAN GOVENDER
School of Mechanical Engineering, University of Kwa-Zulu Natal, King George V Avenue, Durban 4041, South Africa

(Received: 13 April 2004; accepted in final form: 2 September 2004)

Abstract. We investigate the convection amplitude in an infinite porous layer subjected to a vibration body force that is collinear with the gravitational acceleration. The analysis shows that increasing the vibration frequency causes the convection amplitude to approach zero, i.e., increasing the vibration frequency stabilizes the convection.

Key words: vibration, convection, porous media, amplitude.

Nomenclature

Latin Symbols

g^*	acceleration due to gravity.
Fr	Froude number.
H^*	height of the mushy layer.
Da	Darcy number, k_0^*/H^{*2}.
$\hat{e}_z$	unit vector in the z-direction.
k_c	characteristic permeability.
L	length of the mushy layer.
p	reduced pressure.
Pr	Prandtl number, ν^*/κ^*.
R	rescaled Rayleigh number, Ra/π^2.
Ra	Rayleigh number, $\beta_* \Delta T_C g_* k_{c^*} H_*/\nu_* \lambda_*$.
s_x	x-component of wavenumber.
s_y	y-component of wavenumber.
t	time.
T	dimensionless temperature, $(T^* - T_L)/(T_L - T_E)$.
u	horizontal x-component of the filtration velocity.
$\mathbf{V}$	dimensionless filtration velocity vector, $u\hat{e}_x + v\hat{e}_y + w\hat{e}_z$.
v	horizontal y-component of filtration velocity.
w	vertical component of filtration velocity.
$\mathbf{X}$	space vector, $x\hat{e}_x + y\hat{e}_y + z\hat{e}_z$.
x	horizontal length co-ordinate.
y	horizontal width co-ordinate.
z	vertical co-ordinate.

Greek Symbols

α scaled wavenumber, s^2/π^2.
β solutal expansion coefficient.
δ vibration amplitude, $\kappa Fr\Omega^2$.
ε convection amplitude.
ϕ porosity.
κ vibration amplitude, b^*/H^*.
λ thermal diffusivity.
μ dynamic viscosity of the fluid.
ν kinematic viscosity.
ρ fluid density.
Ω vibration frequency.

Superscripts

$*$ dimensional quantities.

Subscripts

0 simplified parameters.
B basic flow quantities.
c characteristic values.
cr critical values.

1. Introduction

Over the past years, interest in fundamental studies of thermal convection in porous media has significantly increased due to its presence in diverse engineering applications. In general buoyancy induced flows in porous media plays an important role in engineering applications. To choose one engineering application, let us consider binary alloy solidification as an example. In the solidification of binary alloys, one finds the presence of three distinct layers viz., the solid layer, the melt layer and the mushy layer, which is sandwiched between the solid and melt regions. The mushy layer may be thought of as a two-phase zone/reactive porous medium that serves to smear the concentration gradient between the solid and melt regions. Experimental studies by Sample and Sarazin (1984) and Sarazin and Hellawell (1998) reveal important information on mechanism for channel formation. It is also demonstrated that the dynamics occurring in the mushy layer are critical to the quality of the final product. Amberg and Homsy (1993), Anderson and Worster (1995) and Worster (1992) provide an excellent numerical analysis of the effects of gravity on solidification, whilst Govender and Vadasz (2002a, b) and Govender (2003) extend their work by proposing rotation as a means of stabilising convection.

Lately Govender (2004) has shown that vibration stabilises convection in a passive porous layer. The objective of the current work is to perform a weak non-linear analysis in order to study the effects of vibration on the convection amplitude, relative to the case of no vibration.

2. Problem Formulation

Govender (2004) presented a detailed formulation of the continuity, energy and Darcy equations (extended to include vibration) for porous media. As the derivation will not be repeated here, readers are referred there for a detailed analysis. The dimensionless governing equations are presented as follows:

$$\nabla \cdot \boldsymbol{V} = 0, \tag{1}$$

$$\left(\frac{1}{Va}\frac{\partial}{\partial t} + 1\right)\boldsymbol{V} = -\nabla p - Ra[1 + \delta \sin(\Omega t)]T\hat{e}_z, \tag{2}$$

$$\frac{\partial T}{\partial t} + \boldsymbol{V} \cdot \nabla T = \nabla^2 T. \tag{3}$$

The symbols $\boldsymbol{V}$, T and p represent the dimensionless filtration velocity vector, temperature and reduced pressure, respectively, and $\hat{e}_z$ is a unit vector in the z-direction. In Equation (2), Ω is the scaled frequency, defined as $\Omega = \omega_* H_*^2/\lambda_*$, whilst the non-dimensional amplitude δ is defined as $\delta = \kappa Fr \Omega^2$, where $\kappa = b_*/H_*$ and Fr is the modified Froude number defined as $Fr = \lambda_*^2/\left(g_* H_*^3\right)$. The parameter Va is the Vadasz number, as pointed out by Straughan (2000), and includes the Prandtl and Darcy numbers as well as the porosity of the porous domain and is defined as $Va = \phi Pr/Da$, where $Pr = \nu_*/\lambda_*$is the Prandtl number, $Da = k_{c^*}/H_*^2$ is the Darcy number, ϕ is the porosity and ν_* stands for the kinematic viscosity of the fluid. It is only through this combined dimensionless group that the Prandtl number affects the flow in the porous media, see Vadasz (1998) for a full discussion on the numerical values that Pr can assume in a typical porous medium. In Equation (2) one also observes the Rayleigh number, Ra; defined as $Ra = \beta_* \Delta T_C g_* k_{c^*} H_*/\nu_* \lambda_*$. As all boundaries are rigid, the solution must follow the impermeability conditions there, i.e., $\boldsymbol{V} \cdot \hat{e}_n = 0$ on the boundaries, where $\hat{e}_n$ is a unit vector normal to the boundary. The temperature boundary conditions are: $T = 1$ at $z = 0$, $T = 0$ at $z = 1$ and $\nabla T \cdot \hat{e}_n = 0$ on all other walls representing the insulation condition on these walls. The partial differential equations (1)–(3) forms a non-linear coupled system which together with the corresponding boundary conditions accepts a basic motionless solution with a parabolic pressure distribution. The solutions for the basic temperature and flow field is given as, $T_B = 1 - z$ and $\boldsymbol{V}_{\mathrm{B}} = 0$.

3. Weak Non-Linear Analysis

The objective of the weak non-linear analysis is to provide quantitative results regarding the amplitude of convection. For subsequent steps it is convenient to use the definition of the stream function in the form

$u = \partial\psi/\partial z$; $w = -\partial\psi/\partial x$, and present Equations (1)–(3) in terms of the stream function and temperature as follows for slow time scale variations,

$$\left(\frac{1}{Va}\frac{\partial}{\partial t}+1\right)\nabla^2\psi + Ra(1+\delta\sin(\Omega t))\frac{\partial T}{\partial x}=0, \tag{4}$$

$$\frac{\partial T}{\partial t}+\frac{\partial\psi}{\partial z}\frac{\partial T}{\partial x}-\frac{\partial\psi}{\partial x}\frac{\partial T}{\partial z}=\nabla^2 T, \tag{5}$$

where the definition of the Laplacian operator is given as $\nabla^2 = \partial^2/\partial x^2 + \partial^2/\partial z^2$. The stream function, temperature and amplitude δ may be expanded in terms of a small parameter ϵ, defined as $\varepsilon = [Ra/Ra_{\mathrm{cr}} - 1]^{1/2}$,as follows:

$$[\psi, T] = [\psi_B, T_B] + \varepsilon[\psi_1, T_1] + \varepsilon^2[\psi_2, T_2] + \varepsilon^3[\psi_3, T_3] + O(\varepsilon^4), \tag{6}$$

$$\delta = \delta_0 + \varepsilon\delta_1 + \varepsilon^2\delta_2 + . \tag{7}$$

The expansion (7) is consistent with the basic solution ($T_B = 1 - z$ and $\boldsymbol{V}_{\mathrm{B}} = 0$) provided that δ_0 vanishes at the lowest order. In addition, unless δ_1 vanishes, the equations obtained at order ε and ε^2 present a singularity in the solution. These observations indicate that the effects of vibration should be introduced at the lowest possible order, i.e., $\delta \approx \varepsilon^2\delta_1$, thereby enabling consistency. By using the definition for ε given above, the Rayleigh number may be expanded as $Ra = Ra_{\mathrm{cr}}(1+\varepsilon^2)$, where $Ra_{\mathrm{cr}} = 4\pi^2$ is the critical Rayleigh number for a porous layer heated from below and subjected to gravity only. In addition we allow time variations only at the slow time scale $\tau = \varepsilon^2 t$ in order to prevent exponential growth and reaching finite values for the amplitude at the steady state. Substituting the expansion (6), as well as the slow time scale, just defined, into the system (4)–(5) and equating like powers of ε produces a hierarchy of linear partial differential equations to each order:

$$\left(\frac{\varepsilon^2}{Va}\frac{\partial}{\partial\tau}+1\right)\nabla^2\psi_{\mathrm{m}} Ra_{\mathrm{cr}}(1+\delta\sin(\Omega_0\tau))\frac{\partial T_{\mathrm{m}}}{\partial x} = H_{\mathrm{m}}, \tag{8}$$

$$\varepsilon^2\frac{\partial T_{\mathrm{m}}}{\partial\tau}+\frac{\partial\psi_{\mathrm{m}}}{\partial z}\frac{\partial T_{\mathrm{m}}}{\partial x}-\frac{\partial\psi_{\mathrm{m}}}{\partial x}\frac{\partial T_{\mathrm{m}}}{\partial z}-\nabla^2 T_{\mathrm{m}} = J_{\mathrm{m}}, \tag{9}$$

where $\Omega_0 = \Omega/\varepsilon^2$ represents the large frequency scaling. To order, ε, $H_1 = J_1 = 0$ and the solution at order ε is given by

$$\psi_1 = A_1\sin(sx)\sin(\pi z), \quad T_1 = B_1\cos(sx)\sin(\pi z). \tag{10}$$

The relationship between the amplitudes is obtained by substituting Equation (10) in the system (8)–(9) and is found to be

$$A_1 = -\pi\frac{(\alpha+1)}{\sqrt{\alpha}}B_1. \tag{11}$$

The amplitude A_1 remains undetermined at this stage, and will be determined from a solvability condition of the order $O(\varepsilon^3)$ equations at order ε^3. The critical Rayleigh number and wavenumber to the leading order are found to be $R_{cr}=4$ and $\alpha_{cr}=1$. The governing equations to order ε^2 are given as,

$$\nabla^2\psi_2 + Ra_{cr}\frac{\partial T_2}{\partial \bar{x}} = 0, \quad \nabla^2 T_2 - \frac{\partial \psi_2}{\partial x} = \frac{\partial \psi_1}{\partial z}\frac{\partial T_1}{\partial x} - \frac{\partial \psi_1}{\partial x}\frac{\partial T_1}{\partial z}, \tag{12}$$

and the solutions to this order are given as,

$$\psi_2 = A_2 \sin(sx)\sin(\pi z), \quad T_2 = B_2\cos(sx)\sin(\pi z) + B_{0,2}\sin(2\pi z),$$
$$B_{0,2} = \sqrt{\alpha}B_1A_1/8. \tag{13}$$

The equations to order ε^3 yields a solvability condition which constrains the amplitude of the solution at order ε and enables its determination. The solvability condition is obtained by decoupling the governing equation at order ε^3 to yield a single non-homogenous partial differential equation for T_3 with corresponding forcing functions which include the $O(\varepsilon)$, and $O(\varepsilon^2)$ solutions as follows,

$$\nabla^4 T_3 + Ra_{cr}\frac{\partial^2 T_3}{\partial x^2} = \frac{\partial H_3}{\partial x} + \nabla^2 J_3, \tag{14}$$

where

$$H_3 = -\left(Ra_{cr}(t)\frac{\partial T_1}{\partial x} + \frac{1}{Va}\frac{\partial \nabla^2\psi_1}{\partial \tau}\right),$$
$$J_3 = \frac{\partial T_1}{\partial \tau} + \frac{\partial \psi_1}{\partial z}\frac{\partial T_2}{\partial x} + \frac{\partial \psi_2}{\partial z}\frac{\partial T_1}{\partial x} - \frac{\partial \psi_1}{\partial x}\frac{\partial T_2}{\partial z} - \frac{\partial \psi_2}{\partial x}\frac{\partial T_1}{\partial z}. \tag{15}$$

Setting the coefficients of the secular terms in Equation (14) to zero, yields the following Ginzburg–Landau equation for the leading order $O(\varepsilon)$ amplitude,

$$\frac{dB}{dt} = \mu_0(1+\delta_1\sin(\Omega t))B - \chi B^3, \tag{16}$$

where $B=\varepsilon B_1$. The following notation is used in Equation (16),

$$\mu_0 = \chi\xi, \quad \chi = \frac{\pi^4\gamma(\alpha+1)^2}{4(\alpha+1+\gamma)}, \quad \xi = \frac{4R_{cr}\alpha}{\pi^2(\alpha+1)^3}\varepsilon^2. \tag{17}$$

Equation (16) is in the form of Bernoulli's differential equation and the solution to this type of equation is of the form,

$$B = \frac{\exp[\mu_0(t-\delta_1/\Omega\cos(\Omega t))]}{[2\chi\int\exp[\mu_0(t-\delta_1/\Omega\cos(\Omega t))]dt + C_1]}, \tag{18}$$

where $B(0) = b_0$ and C_1 is an integration constant. When $\delta_2 \to 0$, the analytical solution to Equation (18) is given as,

$$B = \frac{b_0 \xi^{1/2} e^{\mu_0 t}}{[\xi - b_0^2(1 - e^{2\mu_0 t})]^{1/2}}. \tag{19}$$

When $t \to \infty$, the classic steady state solution is found to be $B = 0$ or $B = b_0/|b_0|\xi^{1/2}$. If $\delta_2 \neq 0$, we observe that the integral in Equation (18) cannot be evaluated to obtain a closed form solution, and it is for this reason that we resort to a numerical solution of Equation (18) by adopting the Runge–Kutta method. Figure 1 shows the numerical versus analytical solution, of amplitude B versus time, for Equation (18) for $\delta_2 = 0$ (no vibration). The results are shown for large Vadasz numbers (i.e., $\gamma \to \infty$) and

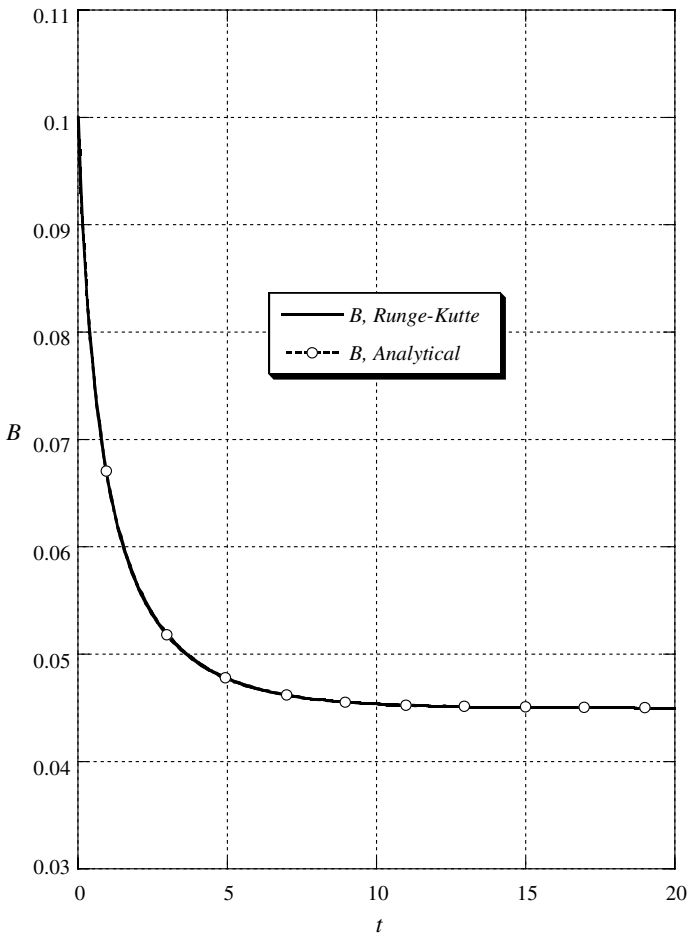

Figure 1. Convection amplitude B versus time for both the numerical and analytical solution for $\delta_2 = 0$.

at an initial amplitude $b_0 = 0.1$, at the critical conditions, i.e., $R_{cr} = 4$ and $\alpha_{cr} = 1$. The results are presented at a time step of 0.079, which will be retained for simulations corresponding to $\delta_2 \neq 0$ in the subsequent figures. Figure 1 clearly shows that there is an excellent agreement between the numerical and analytical solutions for the case of no vibration. Figure 2 shows the amplitude B versus time for $\Omega = 0, 100$ and 250. It can be clearly seen that increasing the frequency from $\Omega = 0$ to 100 reduces the convection amplitude B. For $\Omega = 250$, it can be observed that for $t > \approx 7.5$, the conduction solution ($B = 0$) is stable. Figure 3 shows the amplitude B versus time for $\Omega = 0, 300$ and 350. It can be seen for $\Omega = 300$ that beyond $t \approx 20$ the conduction solution is stable, whilst for $\Omega = 350$, the conduction solution sets in as the stable mode as early as $t \approx 2.5$. Figure 4 shows the

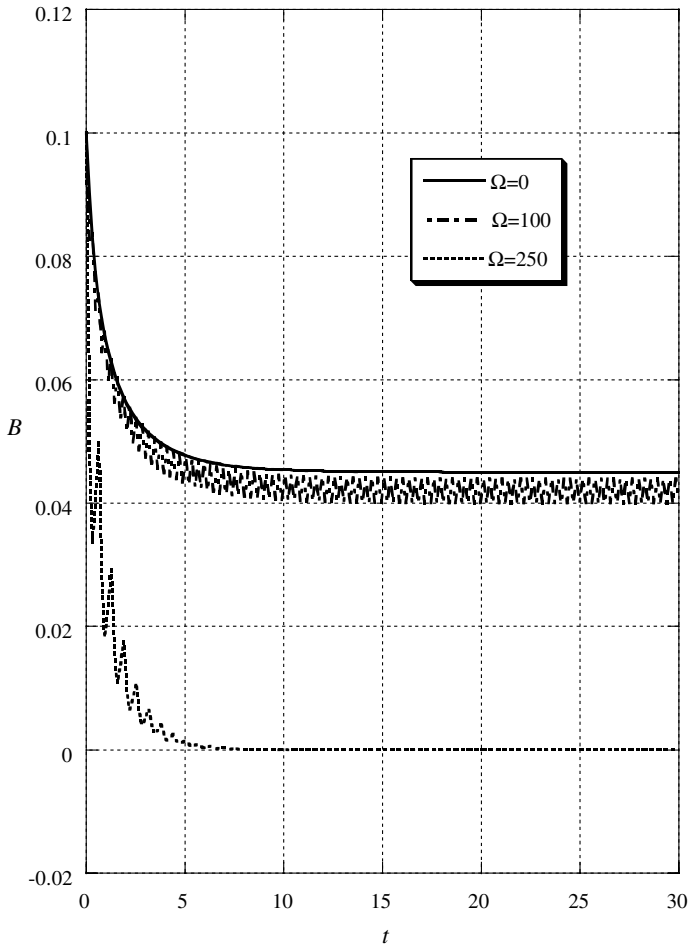

Figure 2. Convection amplitude B versus time for $\Omega = 0, 100$ and 250.

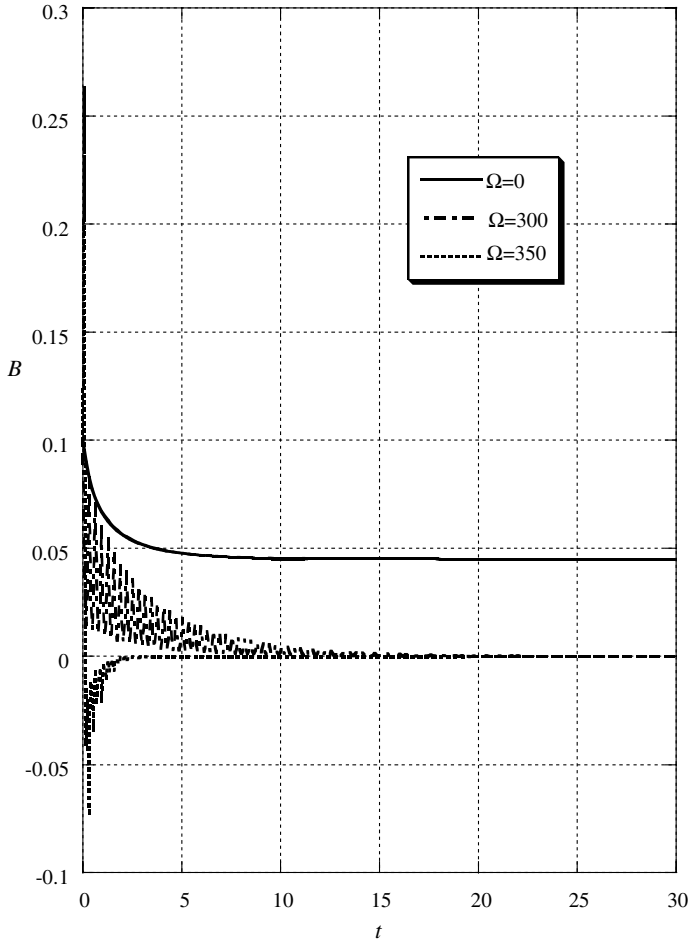

Figure 3. Convection amplitude B versus time for $\Omega = 0, 300$ and 350.

amplitude B versus time for $\Omega = 0, 370$ and 450. Figure 4 shows that the conduction solution is stable beyond $t \approx 5$ for $\Omega = 370$ and 450. Further simulations were performed for $\Omega = 500, 750, 1500$ and 3000, and it was discovered that the basic solution ($B = 0$) is the only possible solution. The results depicted in Figures 2–4 clearly indicate that increasing the vibration frequency stabilizes the convection by causing the convection amplitude to approach zero. These findings have important industrial applications in the solidification of binary alloys say where solutal convection may be suppressed using vibration. It is quite well documented that due to sharp concentration difference between the liquid melt and solid regions, a mushy layer forms in order to smear out the concentration gradient. The dynamics occurring within the mushy layer has an important effect on the ultimate

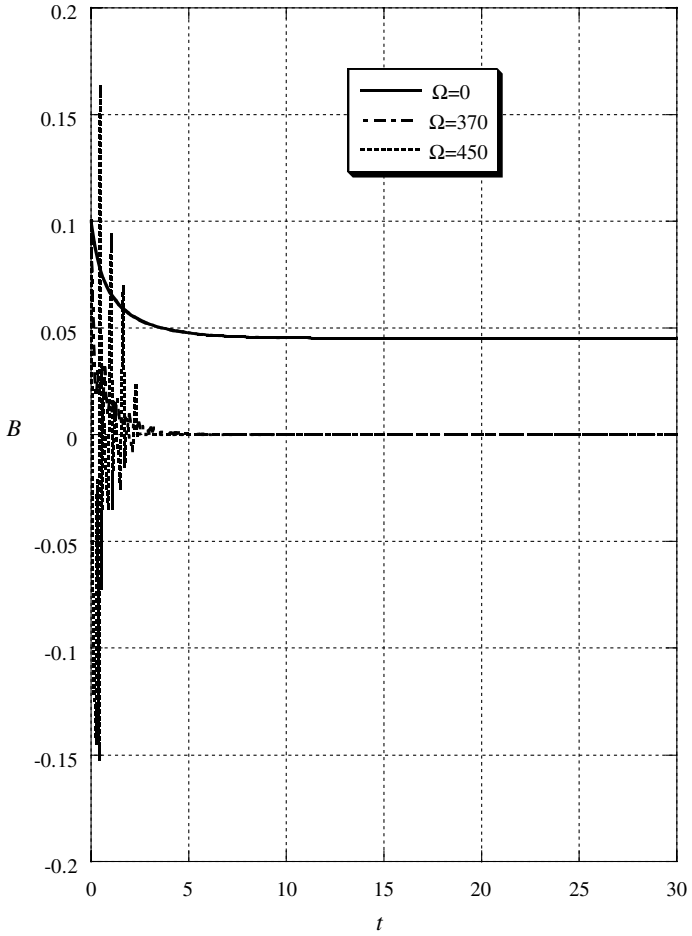

Figure 4. Convection amplitude B versus time for $\Omega = 0, 370$ and 450.

quality of the final ingot and it is widely known that the presence of solutal convection in mushy layers results in the formation of channels, which appear as freckles in cross-section. Vibration can be easily used as an agitation technique in the continuous casting process, whilst the ingot is still in the semi-solid phase, in order to suppress the effects of solutal convection thereby producing a better quality alloy. The linear stability and weak non-linear analysis of solutal convection in mushy layers is a topic that is currently under investigation by the author.

4. Conclusion

Analytical results are presented for convection in a porous layer subjected to vibration and heated from below. A weak non-linear analysis was

performed for an extended Darcy formulation and the numerical results revealed that increasing the frequency of vibration causes the amplitude of convection to approach zero, i.e., vibration stabilises the convection.

Acknowledgements

The author would like to thank the National Research Foundation (NRF) for funding this research through the THUTUKA Program (REDIBA – GUN: 2053945). This paper is dedicated to Bessie (1994–2004), whose presence is sadly missed.

References

Amberg, G. and Homsy, G. M.: 1993, Nonlinear analysis of buoyant convection in binary solidification to channel formation, *J. Fluid Mech*. **252**, 79–98.

Anderson, D. M. and Worster, M. G.: 1995, Weakly non-linear analysis of convection in mushy layers during the solidification of binary alloys, *J. Fluid Mech*. **302**, 307–331.

Govender, S. and Vadasz, P.: 2002a, Weak nonlinear analysis of moderate Stefan number oscillatory convection in rotating mushy layers, *Transp. Porous Media* **48**(3), 353–372.

Govender, S. and Vadasz, P.: 2002b, Weak nonlinear analysis of moderate Stefan number stationary convection in rotating mushy layers, *Transp. Porous Media*, **49**(3), 247–263.

Govender, S.: 2003, On the linear stability of large Stefan number convection in rotating mushy layers for a new Darcy equation formulation, *Transp. in Porous Media* (in press).

Sample, A. K. and Hellawell, A.: 1984, The mechanisms of formation and prevention of channel segregation during alloy solidification, *Metall. Trans. A* **15**A, 2163–2173.

Sarazin, J. R. and Hellawell, A.: 1998, Channel formation in Pb–Sb, and Pb–Sn–Sb alloy ingots and comparison with the system NH_4Cl–H_2O, *Metall. Trans. A* **19**A, 1861–1871.

Vadasz, P.: 1998, Coriolis effect on gravity driven convection in a rotating porous layer heated from below, *J. Fluid Mech*. **376**, 351–375.

Veronis, P.: 1958, Cellular convection with finite amplitude in a rotating fluid. *J. Fluid Mech*. **5**, 401–433.

Worster, M. G.: 1992, Instabilities of the liquid and mushy regions during solidification of alloys, *J. Fluid Mech.* **237**, 649–669.